

WUE-ITP-2004-039
SHEP-04-40

Probing the light neutral Higgs boson scenario of the CP-violating MSSM Higgs sector at the LHC

Dilip Kumar Ghosh^{a,1} and Stefano Moretti^{b,2}

^a *Institut für Theoretische Physik und Astrophysik,
Universität Würzburg, D-97074, Würzburg, Germany*

^b *School of Physics & Astronomy, University of Southampton,
Highfield, Southampton SO17 1BJ, United Kingdom*

Abstract

In the CP-violating Minimal Supersymmetric Standard Model (MSSM), for certain values of the CP-violating phases associated to the universal trilinear couplings (A_t, A_b) and the gluino mass ($M_{\tilde{g}}$), e.g., $\Phi_{\text{CP}} = 60^\circ$ or 90° , for $M_{H^+} \lesssim 140$ GeV and $\tan\beta \sim 2 - 5$, the lightest Higgs boson mass (M_{H_1}) is $\lesssim 50$ GeV. This mass interval is still allowed from standard LEP Higgs searches because of a strongly suppressed $H_1 ZZ$ coupling. However, in the same region of parameter space in which these two conditions occur, the $H_1 H^\mp W^\pm$ coupling is enhanced because the two mentioned sets of couplings satisfy a sum rule. In this paper we probe such a light Higgs scenario at the Large Hadron Collider (LHC) by studying $H^\pm H_1$ associate production, leading to a $4b + \ell^\pm + \cancel{E}_T$ signal. We show that the latter is readily accessible at the CERN hadron collider, upon the application of suitable selection cuts against the Standard Model (SM) backgrounds. Our parton level Monte Carlo (MC) analysis yields $\sim 15 - 45$ signal events, completely free of SM background, for $\mathcal{L} = 10 - 30 \text{ fb}^{-1}$ of accumulated luminosity, after taking into account the overall efficiency for tagging four b -jets.

¹dghosh@physik.uni-wuerzburg.de

²stefano@hep.phys.soton.ac.uk

The experimental observation of Higgs bosons and the determination of their properties is crucial for the understanding of Electro-Weak Symmetry Breaking (EWSB). Thus, the search for Higgs bosons is one the major goals of the present collider Tevatron (Run II) and future ones as well, such as the forthcoming LHC and the planned International Linear Collider (ILC). In the SM, the Higgs boson mass is not predicted. Over the last few decades, many efforts have been put into detecting such a particle, but to no avail. From direct searches at LEP, a lower bound of 114 GeV has been set on its mass [1, 2]. In the MSSM, with all real and CP-conserving parameters, the lower limit on the lightest Higgs boson is ~ 90 GeV [3] for any $\tan \beta$. However, this bound is significantly lowered in an MSSM scenario with radiatively induced Higgs sector CP-violation, as the latter in turn implies a suppressed $H_1 ZZ$ coupling [4].

CP-violation in the Higgs sector is possible in multi-Higgs doublet models, such as a general 2-Higgs Doublet Model (2HDM) or indeed the MSSM. In the latter, it has been shown that, assuming universality of the gaugino masses ($M_i, i = 1, 2, 3$) at some high energy scale, the CP-violating MSSM Higgs sector can be parametrised in terms of two independent phases: that of the Higgsino mass parameter (also called μ term), i.e., $\text{Arg}(\mu)$, and that of the soft trilinear Supersymmetry (SUSY) breaking parameters, i.e., $\text{Arg}(A_f)$, with $f = t, b$. The experimental upper bounds on the Electric Dipole Moments (EDMs) of electrons and neutrons (EDMs) [5, 6] as well as of mercury atoms [7] may pose severe constraints on these phases. However, these limits are highly model dependent. In particular, it has been shown that one could still have large CP-violating phases yielding relevant EDM values all satisfying current experimental bounds if any of these three possibilities is realised: (a) the sfermions of the first two generations are heavy, of the order of a few TeV [8]; (b) cancellations between different EDM contributions [9] take place; (c) universality of the trilinear scalar couplings A_f is dismissed [10, 11]. However, only in the scenario with first and second generation sfermions much heavier than the third generation ones, the phase of μ can be large. Otherwise, it is strongly constrained, as $\text{Arg}(\mu) \lesssim 10^{-2}$.

In the MSSM, non-zero phases of μ and/or the trilinear scalar couplings A_f can induce CP-violation at one-loop level in the Higgs sector even in presence of a CP-conserving tree-level scalar potential, through the CP-violating interactions among Higgs bosons and heavy sfermions. This one-loop corrected Higgs potential then generates non-zero off-diagonal terms \mathcal{M}_{SP}^2 in the 3×3 neutral Higgs boson mass-squared matrix \mathcal{M}_{ij}^2 , representing mixing between CP-even (or scalar, S) and CP-odd (or pseudoscalar, P) states [12]–[17]. These off-diagonal entries can approximately be written as follows [13]:

$$\mathcal{M}_{SP}^2 \approx \mathcal{O} \left(\frac{M_t^4 |\mu| |A_t|}{v^2 32\pi^2 M_{\text{SUSY}}^2} \right) \sin \Phi_{\text{CP}} \left[6, \frac{|A_t|^2}{M_{\text{SUSY}}^2}, \frac{|\mu|^2}{\tan \beta M_{\text{SUSY}}^2}, \frac{\sin 2\Phi_{\text{CP}} |A_t| |\mu|}{\sin \Phi_{\text{CP}} M_{\text{SUSY}}^2} \right], \quad (1)$$

where $\Phi_{\text{CP}} = \text{Arg}(A_t) = \text{Arg}(\mu)$ and $v = 246$ GeV. The mass scale M_{SUSY}^2 is typically defined to be $(m_{\tilde{t}_1}^2 + m_{\tilde{t}_2}^2)/2$, i.e., in terms of the two stop masses. After diagonalizing the 3×3 symmetric Higgs mass-squared matrix \mathcal{M}_{ij}^2 by an orthogonal matrix O , the physical mass eigenstates H_1, H_2 and H_3 (in ascending order of mass) are states of indefinite CP-parity. In this case, M_{H^\pm} is the most appropriate mass parameter to describe the MSSM Higgs-sector (in place of M_A , often used in the CP-conserving case).

The CP-violating phases can cause the Higgs couplings to fermions and gauge bosons to change significantly from their tree-level values, with dramatic consequences for MSSM Higgs phenomenology at present and future colliders [18]. Here, we start by presenting the form of the MSSM couplings $H_i VV$, $H_i H_j Z$ and $H_i H^- W^+$, where $V = W^\pm, Z$, in presence of explicit CP-violation³:

$$\mathcal{L}_{H_i VV} = g m_W \sum_{i=1}^3 g_{H_i VV} [H_i W_\mu^+ W^{-\mu} + \frac{1}{2c_W^2} H_i Z_\mu Z^\mu], \quad (2)$$

$$\mathcal{L}_{H_i H_j Z} = \frac{g}{2c_W} \sum_{j>i=1}^3 g_{H_i H_j Z} (H_i \overset{\leftrightarrow}{\partial}_\mu H_j) Z^\mu, \quad (3)$$

$$\mathcal{L}_{H_i H^- W^+} = \frac{g}{2c_W} \sum_{i=1}^3 g_{H_i H^- W^+} (H_i \overset{\leftrightarrow}{\partial}_\mu H^-) W^{+\mu}, \quad (4)$$

where

$$g_{H_i VV} = O_{1i} \cos \beta + O_{2i} \sin \beta, \quad (5)$$

$$g_{H_i H_j Z} = O_{3i} (\cos \beta O_{2j} - \sin \beta O_{1j}) - (i \leftrightarrow j), \quad (6)$$

$$g_{H_i H^- W^+} = O_{2i} \cos \beta - O_{1i} \sin \beta + i O_{3i}. \quad (7)$$

These couplings obey the following sum rules:

$$\sum_{i=1}^3 g_{H_i VV}^2 = 1, \quad (8)$$

$$g_{H_i VV}^2 + |g_{H_i H^- W^+}|^2 = 1, \quad (9)$$

$$g_{H_k VV} = \epsilon_{ijk} g_{H_i H_j Z}. \quad (10)$$

Hence, from the above formulae, one can see that – if two of the $g_{H_i ZZ}$ are known – then the whole set of couplings between neutral Higgs bosons and gauge bosons is determined. It is also interesting to see from Eq. (9) that – in the presence of large CP violating effects with large scalar-pseudo-scalar mixing – a suppressed $H_1 VV$ coupling means an enhanced strength of the $H_1 H^- W^+$ vertex, as intimated already. This enhancement will indeed play a significant role in our analysis. Equally important is the correlation between the mass of the charged Higgs state, M_{H^\pm} , and that of the pseudo-scalar state, M_A . In fact, a suppressed $H_1 VV$ coupling implies a light pseudo-scalar state which in turn leads to a light charged Higgs, in particular $M_{H^\pm} < m_t$ (the top quark mass).

From Eq. (1), it is clear that sizeable scalar-pseudo-scalar mixing is possible for a large value of the CP-violating phase Φ_{CP} and/or of $|\mu|$ and $|A_t|$. In this respect, the CP-violating benchmark scenario defined as CPX in [13] provides a suitable choice of MSSM parameters which maximizes CP-violating effects and can then be used to study the most striking phenomenological manifestations of explicit CP-violation in the MSSM Higgs sector. Such a scenario is

³Further details can be found in Ref. [13].

defined as followed:

$$M_{\tilde{Q}} = M_{\tilde{t}} = M_{\tilde{b}} = M_{\text{SUSY}}, \quad (11)$$

$$\mu = 4M_{\text{SUSY}}, \quad |A_t| = |A_b| = 2M_{\text{SUSY}}, \quad (12)$$

$$\text{Arg}(A_t) = \text{Arg}(A_b). \quad (13)$$

Recently, the OPAL Collaboration [19] reported their results for Higgs boson searches in a CP violating MSSM Higgs sector using the parameters defined in the CPX scenario and found that for the CP-violating phases $\Phi_{\text{CP}} = 60^\circ$ and 90° and certain values of M_{H^\pm} and $\tan \beta$, the lowest mass limit on the neutral Higgs is very light – at times even vanishing completely – hence resulting in some low Higgs mass windows in the M_{H^\pm} – $\tan \beta$ plane which are still allowed by LEP data. In a nutshell, the reason for the existence of such regions is the fact that in the CPX scenario the lightest Higgs boson is almost CP-odd with highly suppressed couplings to ZZ pairs.

The experimental analysis was done by adopting both CPSuperH [20] and FeynHiggs 2.0 [21], as these are the two public codes available for the calculation of masses and mixing angles in the CP-violating MSSM Higgs sector. In reality, these two programs give somewhat different results – at least in the case of the CPX scenario – mainly due to different approximations used in their calculations. To give more conservative constraints, the experimentalists used the lower prediction of the two for the expected Higgs boson cross-sections. The constraints also depend sensitively on the mass of the top quark used in the calculation [3]⁴. The results of [3], from a combined analysis of all LEP data, provide exclusion regions in the M_{H_1} – $\tan \beta$ plane for the following values of the SUSY parameters:

$$\text{Arg}(A_t) = \text{Arg}(A_b) = \text{Arg}(M_{\tilde{g}}) = \Phi_{\text{CP}}, \quad (14)$$

$$M_{\text{SUSY}} = 0.5 \text{ TeV}, \quad M_{\tilde{g}} = 1 \text{ TeV}, \quad (15)$$

$$M_{\tilde{B}} = M_{\tilde{W}} = 0.2 \text{ TeV}, \quad (16)$$

$$\Phi_{\text{CP}} = 0^\circ, 30^\circ, 60^\circ, 90^\circ, \quad (17)$$

where, $M_{\tilde{B}}$, $M_{\tilde{W}}$ and $M_{\tilde{g}}$ represent the soft SUSY-breaking masses for bino, wino and gluino.

By combining the results of Higgs searches from ALEPH, DELPHI, L3 and OPAL, the authors of Ref.[22] also provided exclusion regions in the M_{H_1} – $\tan \beta$ (as well as M_{H^\pm} – $\tan \beta$) plane for the same set of parameters. The exact shape of the exclusion regions may be somewhat different in their analyses, but they all show that for certain values of CP-violating phases LEP cannot rule out a light Higgs mass at low values of $\tan \beta$. This interesting situation roughly corresponds to $\tan \beta \sim 3.5 - 5$, $M_{H^\pm} \sim 125 - 140$ GeV (yielding $M_{H_1} \lesssim 50$ GeV) and $\tan \beta \sim 2 - 3$, $M_{H^\pm} \sim 105 - 130$ GeV (yielding $M_{H_1} \lesssim 40$ GeV), respectively. The authors of Ref. [22] further showed that in the same regions the $H_1 t\bar{t}$ coupling is suppressed too. Thus, these two particular areas of the parameter space can be probed neither at the Tevatron – where the associated production WH_1 mode is the most promising one – nor at the LHC – as

⁴They were obtained for $m_t = 175$ GeV, the value we adopt here.

the reduced $H_1 t\bar{t}$ coupling suppresses both the inclusive production mode $gg \rightarrow H_1$ and the associated one $t\bar{t}H_1$.

We have however found that, in the mentioned regions of the $M_{H^\pm} - \tan \beta$ plane, the decay $H^\pm \rightarrow H_1 W^\pm$ has a very large ($\sim 100\%$) Branching Ratio (BR), thanks to the discussed enhancement of the $H^\mp H_1 W^\pm$ coupling and the mass hierarchy $m_t > M_{H^\pm} \gg M_{H_1}$. This feature motivated us to then study the possibility of probing such a light Higgs scenario in the CP-violating MSSM Higgs model through the process $pp \rightarrow H_1 H^\pm \rightarrow H_1 (H_1 W^\pm) \rightarrow b\bar{b}b\bar{b}\ell\nu$ at LHC. Recently in Ref.[23] the authors have probed this light Higgs scenario through $t\bar{t}$ production at the LHC, where one of the top quark decays into $b\bar{b}W$ channel, via $t \rightarrow bH^\pm, H^\pm \rightarrow W^\pm H_1$ and $H_1 \rightarrow b\bar{b}$ leading to $4b + jj + \ell^\pm + \cancel{E}_T$ signal. In our analysis, the signal will consist of up to four b -jets along with a hard lepton (electron or muon) and missing transverse energy \cancel{E}_T , according to the following decay pattern:

$$\begin{array}{ccccc}
 pp \rightarrow & H^+ & + & H_1 & + & X \\
 & \swarrow & & \swarrow & & \\
 & W & & H_1 & & b\bar{b} \\
 & \swarrow & & \swarrow & & \\
 & \ell\nu & & b\bar{b} & &
 \end{array}$$

In short, such a production and decay mechanism should allow to probe the possible existence of a light H_1 state in the above mentioned two interesting windows of the CP-violating MSSM in the CPX scenario. The production mechanism $pp \rightarrow H^\pm W^\mp$ was discussed in Ref. [24], but no decay and phenomenological analyses where reported there.

Our numerical results are obtained from a parton level MC analysis, wherein partons are treated as jets and the latter are isolated according to a standard cone algorithm. As acceptance and selection criteria we required:

1. $|\eta| < 2.5$ for all jets and leptons, where η denotes pseudo-rapidity;
2. $p_T^{b\text{-jets}} > 15$ GeV;
3. $p_T^\ell > 10$ GeV ($\ell = e, \mu$);
4. $\cancel{E}_T > 20$ GeV;
5. a minimum separation $\Delta R \equiv \sqrt{(\Delta\phi)^2 + (\Delta\eta)^2} = 0.4$ between leptons and jets as well as each pair of jets;
6. reconstruction of the two light Higgs bosons, by requiring four b 's in the event to be tagged as such⁵ and that at least one out of the three possible double pairings of b -jets

⁵With no jet- and/or lepton-charge determination, though.

satisfies the following mass constraint:

$$\frac{(m_{b_1,b_2} - M_{H_1})^2 + (m_{b_3,b_4} - M_{H_1})^2}{\sigma_m^2} < 2, \quad (18)$$

where $\sigma_m = 0.12 M_{H_1}$.

(In enforcing the latter constraint, we implicitly assume that trial values for M_{H_1} are attempted and the selection has hit on the right one.) Notice that we impose Gaussian smearing on energies, with $\Delta E/E = 0.6/\sqrt{E}$ for jets and $\Delta E/E = 0.12/\sqrt{E}$ for leptons, to realistically emulate finite experimental resolution. All such cuts and smearing procedure have been applied to any process studied in this paper, alongside using CTEQ(5L) [26] as Parton Distribution Functions (PDFs) taken at the scale $Q^2 = \hat{s}$ (same for the scale of α_S , where relevant).

In Figure 1 we show the variation of the signal cross-section (including the suppression due to a quadruple b -tagging efficiency, $\epsilon_b^4 = (1/2)^4 = 1/16$ with M_{H^\pm} [(a) and (b)] and M_{H_1} [(c) and (d)] for the CP-violating phase choices $\Phi_{\text{CP}} = 60^\circ$ [(a) and (c)] and 90° [(b) and (d)], respectively, for three values of $\tan\beta$. The choice of other MSSM parameters is defined through Eqs. (14)–(16). We have used the CPSuperH program [20] with $m_t = 175$ GeV to calculate the masses, couplings and decay rates of the relevant Higgs bosons and semi-analytical techniques to evaluate the hadro-production cross-section and decay rates. From Figure 1(a) and (b) one can see that the signal cross-section has a peculiar dependence upon M_{H^\pm} . This may seem counter-intuitive, as the light Higgs mass increases with increasing M_{H^\pm} . However, it should be noticed that, at lower M_{H_1} values, the b -jets emerging from the Higgs decays are rather soft and close to each other in phase space. As the light Higgs mass increases though, b -jets become harder and also acquire much larger angular separations, hence a kinematics satisfying the cuts mentioned above more often, counter-balancing the decline in production rates due to larger M_{H_1} values, ultimately leading to an overall relative rise in the cross-section. The final drop in the latter is due to phase space suppression for the $H^\pm \rightarrow H_1 W^\pm$ decay. In this scenario the largest cross-section, ~ 1.36 fb, can be obtained for $\Phi_{\text{CP}} = 60^\circ$, $\tan\beta = 2$ and $M_{H^\pm} \sim 130$ GeV, which corresponds to $M_{H_1} \sim 40$ GeV. For the CP violating phase $\Phi_{\text{CP}} = 90^\circ$, the largest cross-section, ~ 1.5 fb, can be obtained for $\tan\beta = 4$ and $M_{H^\pm} \sim 139$ GeV, which corresponds to $M_{H_1} \sim 50$ GeV. From Figure 1(b) and (d), it is interesting to notice that the cross-section is almost insensitive to $\tan\beta$ at low values of M_{H_1} .

The SM background cross-section for this signal arising from⁶

1. QCD production of $gg \rightarrow b\bar{b}jj\ell\nu$;
2. Electro-Weak (EW) $q\bar{q}' \rightarrow ZZ W^\pm$ production, followed by the decay of each Z into $b\bar{b}$ pairs and by electron/muon decays of the W -boson;
3. top-quark production and decay via $gg \rightarrow t\bar{t} \rightarrow b\bar{b}jj\ell\nu$;

⁶Hereafter, j labels both light (u, d, s, c) and heavy (b) quark jets.

is not shown, as it is negligible. In fact, after applying the same cuts 1.–6. to both signal and background processes and folding the cross-sections with the usual b -tagging efficiency ($\epsilon_b = 1/2$) and the appropriate light-quark jet rejection factors (assuming $R_{u,d,s} = 1/50$ and $R_c = 1/25$) [25], we found that

1. $\sigma(gg \rightarrow b\bar{b}jj\ell\nu) \lesssim 2.2 \times 10^{-3} \text{ fb};$
2. $\sigma(q\bar{q}' \rightarrow ZZW^\pm \rightarrow b\bar{b}jj\ell\nu) \lesssim 4.0 \times 10^{-3} \text{ fb};$
3. $\sigma(gg \rightarrow t\bar{t} \rightarrow b\bar{b}jj\ell\nu) \lesssim 2.9 \times 10^{-2} \text{ fb};$

where we have taken into account all relevant Z, W^\pm BRs and combinatorial factors.

In Ref. [22], the authors discussed $q\bar{q}' \rightarrow H_2 W^\pm$ as another possible probe of CP-violation in the MSSM Higgs sector, wherein $W^\pm \rightarrow \ell\nu$ and $H_2 \rightarrow H_1 H_1 \rightarrow b\bar{b}b\bar{b}$. This mode can then lead to the same signature as the one we have been considering. Hence, one should in principle worry about its numerical relevance as well as possible interference effects between the two channels. In practice though, the $q\bar{q}' \rightarrow H_2 W^\pm \rightarrow H_1 H_1 W^\pm \rightarrow b\bar{b}b\bar{b}\ell\nu$ production and decay rates are much smaller than those for $q\bar{q}' \rightarrow H_1 H^\pm \rightarrow H_1 H_1 W^\pm \rightarrow b\bar{b}b\bar{b}\ell\nu$. This is clearly confirmed by Figure 2. This is also the case for the interference. Therefore, hereafter, we will neglect considering the $q\bar{q}' \rightarrow H_2 W^\pm$ channel further.

Note that signal events will be very striking due to the clustering of two pairs of $b\bar{b}$ invariant masses around M_{H_1} . This feature will of course not be present in the backgrounds, so it can be used to enhance the former and suppress the latter. One can attempt to reconstruct the light Higgs mass in the following ways. Out of the $4b$ final state, one can simply plot all possible (six) combinations of invariant masses $m_{b\bar{b}}$ (each with identical weight). This leads to the signal and background ‘average’ $m_{b\bar{b}}$ distributions appearing in Figure 3(a). Alternatively, one can construct the three possible double pairings of $b\bar{b}$ invariant masses, then select the pair giving the least difference between the two $m_{b\bar{b}}$ values, and the best reconstructed H_1 mass is the corresponding mean value of that pair. This ‘best reconstructed’ $m_{b\bar{b}}$ distribution is shown in Figure 3(b). By comparing the spectra in Figures 3(a) and 3(b), it is clear that the second procedure is more efficient than the first one in increasing the signal-to-background rate. (Hence, we have exploited it by adopting the mass constraint described in Eq. (18).) For the two discussed mass spectra, two sample values of the light Higgs boson mass are assumed in the signal. Also note the normalisation to unity for all processes considered. Naturally, in producing these plots, we have refrained from applying cut 6. above. Figures 3(a) and 3(b) clearly highlight the H_1 resonant peaks for the signal and the Z ones for the EW background. As for the other two background processes, the QCD reveals a typical Jacobian shape, owing to the absence of heavy particles decaying hadronically, while the $t\bar{t}$ one displays W^\pm resonance effects, when two light quarks are mistagged as b -jets. In all cases, it is worth noting that the Gaussian smearing we have applied to the momenta somewhat affect the actual locations of the resonant peaks (where relevant). Under any circumstances, it is clear from both figures that the low mass signal resonances are always located far away from the bulk of all background events appearing at high mass.

The question now arises of whether it is also possible to reconstruct the H^\pm mass in the signal. Because of the presence of a neutrino escaping detection in the $W^\pm \rightarrow \ell\nu$ decay, the actual charged Higgs resonance is not kinematically accessible. Besides, only one of the two $b\bar{b}$ pairs selected via Eq. (18) actually comes from a $H^\pm \rightarrow H_1 W^\pm \rightarrow b\bar{b} W^\pm$ decay chain. In order to obviate such potential problems, we have proceeded as follows. Firstly, by running our MC for the signal, we have verified that the two (hereafter, ‘primary’) b ’s emerging from the decay of the H_1 boson produced in the hard scattering in association with the charged Higgs boson have normally a higher energy than the two produced in the mentioned decay chain (hereafter, ‘secondary’). This is evident from Figure 4, obtained after all cuts 1.–6. have been enforced. Hence, it makes sense to identify, between the two $b\bar{b}$ pairs selected via Eq. (18), the one with least total energy as the one produced in the mentioned H^\pm decay chain. Secondly, we have defined the transverse mass, M_T , constructed from, on the one hand, the visible transverse momentum of the system formed by the ‘secondary’ $b\bar{b}$ pair plus the lepton and, on the other hand, the missing energy, i.e.,

$$M_T = \sqrt{\left(p_T^b + p_T^{\bar{b}} + p_T^\ell + \not{p}_T\right)^2 - \left(\mathbf{p}_T^b + \mathbf{p}_T^{\bar{b}} + \mathbf{p}_T^\ell + \not{\mathbf{p}}_T\right)^2}, \quad (19)$$

where quantities in boldface refer to three-vectors. Such a variable is sensitive, as clearly evident from Figure 5, to the underlying charged Higgs boson mass and thus can be used within a MC simulation to fit the latter.

In summary, we have proved the feasibility of testing at the LHC light Higgs boson windows in the so-called CPX scenario of the CP-violating MSSM, wherein a H_1 signal might have been lost at LEP due to a strongly suppressed $H_1 ZZ$ coupling. Specifically, we have concentrated upon the following two MSSM parameter space regions: (i) $3.5 < \tan\beta < 5$, $M_{H_1} \lesssim 50$ GeV and (ii) $2 < \tan\beta < 3$, $M_{H_1} \lesssim 40$ GeV, assuming a common CP-violating phase $\Phi_{\text{CP}} = 90^\circ$ and 60° , respectively. We have found that, in the above mentioned parameter space areas, a light charged Higgs boson ($M_{H^\pm} < m_t$) can decay to $W^\pm H_1$ pairs with large a branching fraction so that, combined with a sizeable $H^\pm H_1$ associate production rate, the yield of the emerging signature $4b + \ell^\pm + \not{E}_T$ is sufficient to isolate a CP-violating signal. signal events, completely free of SM background, for $\mathcal{L} = 10 - 30 \text{ fb}^{-1}$ of accumulated luminosity, after taking into account the efficiency for tagging all four b -jets. Furthermore, we have also discussed the possibility of measuring the light Higgs boson mass as well as the charged Higgs boson one. We expect that the parton level study presented in this paper will encourage the CMS and ATLAS collaborations to carry out further investigations of the MSSM in presence of explicit CP-violation in the Higgs sector.

Acknowledgements

The work of DKG is supported by the Bundesministerium für Bildung und Forschung Germany, grant 05HT1RDA/6. DKG would also like to thank A. Datta and T. Binoth for discussions.

References

- [1] S. Eidelman *et al.* [Particle Data Group Collaboration], Phys. Lett. B **592** (2004) 1 (see also <http://pdg.lbl.gov>).
- [2] LEP Higgs Working Group, Phys. Lett. B **565**, 61 (2003); CERN-EP-2003-011.
- [3] See: LEP SUSY Working Group, <http://lepsusy.web.cern.ch/lepsusy>, and LEP Higgs Working Group, LHWG-Note 2004-01.
- [4] J. F. Gunion, B. Grzadkowski, H. E. Haber and J. Kalinowski, Phys. Rev. Lett. **79**, 982 (1997).
- [5] P. Nath, Phys. Rev. Lett. **66**, 2565 (1991); Y. Kizukuri and N. Oshimo, Phys. Rev. D **46**, 3025 (1992); T. Ibrahim and P. Nath Phys. Lett. B **418**, 98 (1998); Phys. Rev. D **57**, 478 (1998); *ibid* D **58**, 019901(E) (1998); *ibid* D **60**, 079903 (1999); *ibid* D **60**, 119901 (1999); M. Brhlik, G.J. Good and G.L. Kane, Phys. Rev. D **59**, 115004 (1999); A. Bartl, T. Gajdosik, W. Porod, P. Stockinger and H. Stremnitzer, Phys. Rev. D **60**, 073003 (1999); D. Chang, W.-Y. Keung and A. Pilaftsis, Phys. Rev. Lett. **82**, 900 (1999); S. Pokorski, J. Rosiek and C.A. Savoy, Nucl. Phys. B **570**, 81 (2000); E. Accomando, R. Arnowitt and B. Dutta, Phys. Rev. D **61**, 115003 (2000); S. Abel, S. Khalil and O. Lebedev, Nucl. Phys. B **606**, 151 (2001); U. Chattopadhyay, T. Ibrahim and D.P. Roy, Phys. Rev. D **64**, 013004 (2001); D.A. Demir, M. Pospelov and A. Ritz, hep-ph/0208257.
- [6] A. Pilaftsis, Nucl. Phys. B **644**, 263 (2002).
- [7] T. Falk, K.A. Olive, M. Pospelov and R. Roiban, Nucl. Phys. B **60**, 3 (1999).
- [8] Y. Kizukuri and N. Oshimo in Ref. [5].
- [9] T. Ibrahim *et al.* and M. Brhlik, *et al.* in Ref. [5].
- [10] S. Abel and J.-M. Frere, Phys. Rev. D **55**, 1623 (1997).
- [11] D. Chang *et al.* in Ref. [5].
- [12] A. Pilaftsis, Phys. Rev. D **58**, 096010 (1998); Phys. Lett. B **435**, 88 (1998).
- [13] A. Pilaftsis and C.E.M. Wagner, Nucl. Phys. B **553**, 3 (1999).
- [14] D.A. Demir, Phys. Rev. D **60**, 055006 (1999).
- [15] S.Y. Choi, M. Drees and J.S. Lee, Phys. Lett. B **481**, 57 (2000).
- [16] M. Carena, J.R. Ellis, A. Pilaftsis and C.E.M. Wagner, Nucl. Phys. B **586**, 92 (2000).
- [17] G.L. Kane and L.-T. Wang, Phys. Lett. B **488**, 383 (2000).

- [18] A. Dedes and S. Moretti, Phys. Rev. Lett. **84**, 22 (2000); Nucl. Phys. B **576**, 29 (2000); S.Y. Choi, K. Hagiwara and J.S. Lee, Phys. Rev. D **64**, 032004 (2001); Phys. Lett. B **529**, 212 (2002); A. Arhrib, D.K. Ghosh and O.C.W. Kong, Phys. Lett. B **537**, 217 (2002); S.Y. Choi, M. Drees, J.S. Lee and J. Song, Eur. Phys. J. C **25**, 307 (2002).
- [19] G. Abbiendi *et al.* [OPAL Collaboration], Eur. Phys. J. C **37**, 49 (2004).
- [20] J.S. Lee, A. Pilaftsis, M. Carena, S.Y. Choi, M. Drees, J.R. Ellis and C.E.M. Wagner, Comput. Phys. Commun. **156**, 283 (2004).
- [21] S. Heinemeyer, Eur. Phys. J. C **22**, 521 (2001); M. Frank, S. Heinemeyer, W. Hollik and G. Weiglein, arXiv:hep-ph/0212037.
- [22] M. Carena, J.R. Ellis, S. Mrenna, A. Pilaftsis and C.E.M. Wagner, Nucl. Phys. B **659**, 145 (2003).
- [23] D. K. Ghosh, R.M. Godbole and D.P. Roy, arXiv:hep-ph/0412193.
- [24] A.G. Akeroyd, Phys. Rev. D **68**, 077701 (2003).
- [25] ATLAS, *Technical Proposal for a General-Purpose pp Experiment at the Large Hadron Collider at CERN*, CERN/LHCC/94-43, December, 1994.
- [26] H.L. Lai, J. Huston, S. Kuhlmann, J. Morfin, F. Olness, J.F. Owens, J. Pumplin and W. K. Tung, Eur. Phys. J. C **12**, 375 (2000).

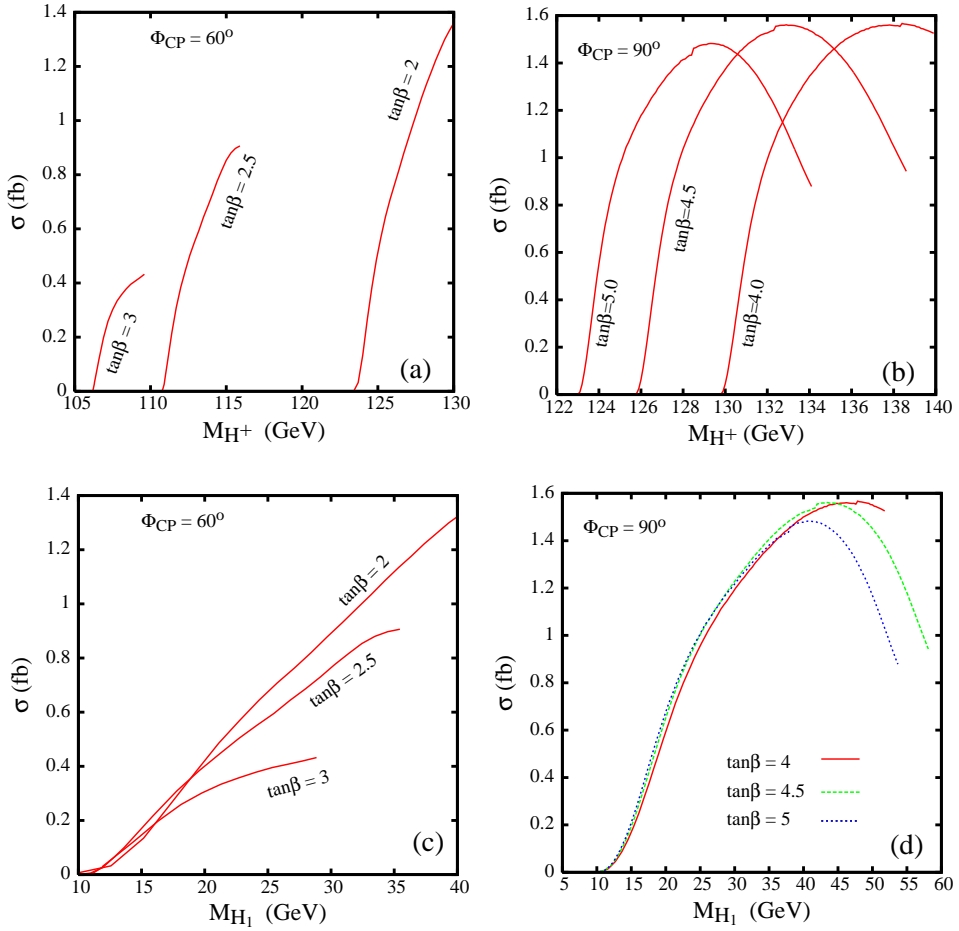


Figure 1: Variation of the signal cross-section with M_{H^\pm} [(a), (b)] and M_{H_1} [(c), (d)] for the two values of CP-violating phases $\Phi_{CP} = 60^\circ$ [(a), (c)] and $\Phi_{CP} = 90^\circ$ [(b), (d)]. The choices of $\tan\beta$ for each CP-violating phase are shown in the figure.

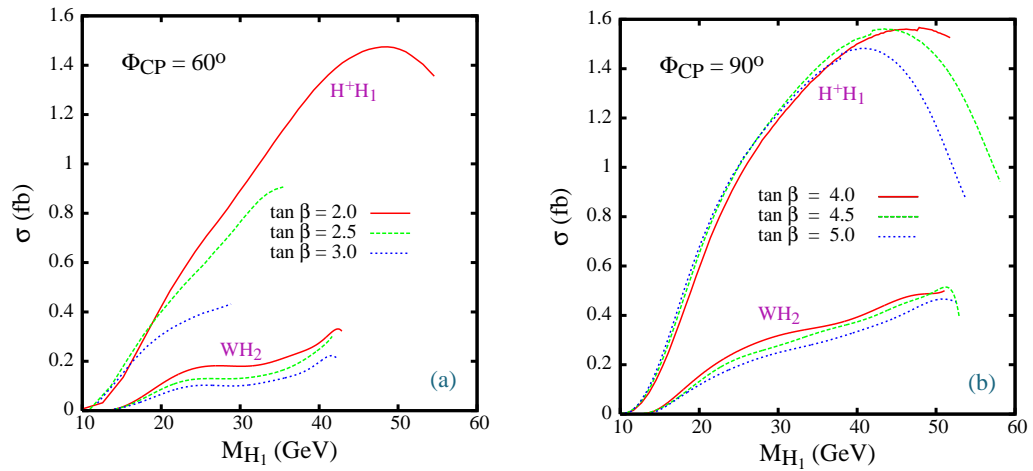


Figure 2: A comparison between the production rates of the two processes $q\bar{q}' \rightarrow H_2 W^\pm \rightarrow H_1 H_1 W^\pm \rightarrow b\bar{b} b\bar{b} \ell\nu$ and $q\bar{q}' \rightarrow H_1 H^\pm \rightarrow H_1 H_1 W^\pm \rightarrow b\bar{b} b\bar{b} \ell\nu$, for $\Phi_{CP} = 60^\circ$ (a) and $\Phi_{CP} = 90^\circ$ (b), for the three choices of $\tan\beta$ shown in the figure.

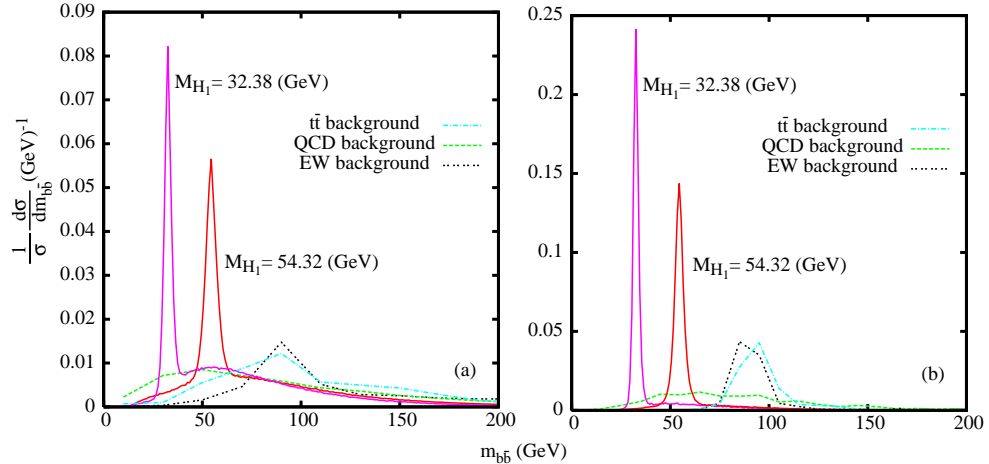


Figure 3: The ‘average’ (a) and ‘best reconstructed’ (b) $m_{b\bar{b}}$ distributions (as described in the text) for the signal (with $M_{H_1} = 32.38$ and 54.32 GeV, corresponding to $M_{H^\pm} = 129.55$ and 136.97 GeV, respectively, for $\tan\beta = 4.5$ and $\Phi_{\text{CP}} = 90^\circ$). The corresponding SM model background distributions are also shown.

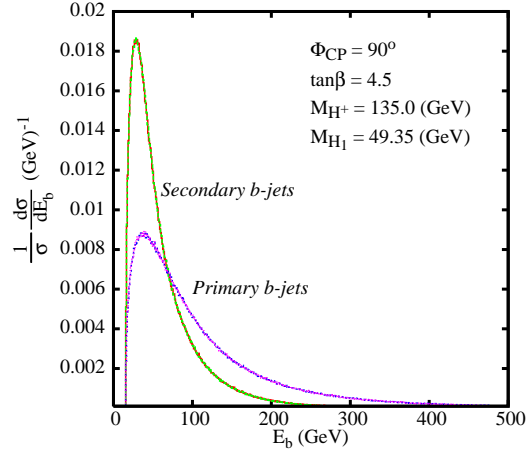


Figure 4: The energy distributions of the two ‘primary’ and two ‘secondary’ b -jets in the signal (as defined in the text), as obtained for the representative parameter choices shown inside the figure.

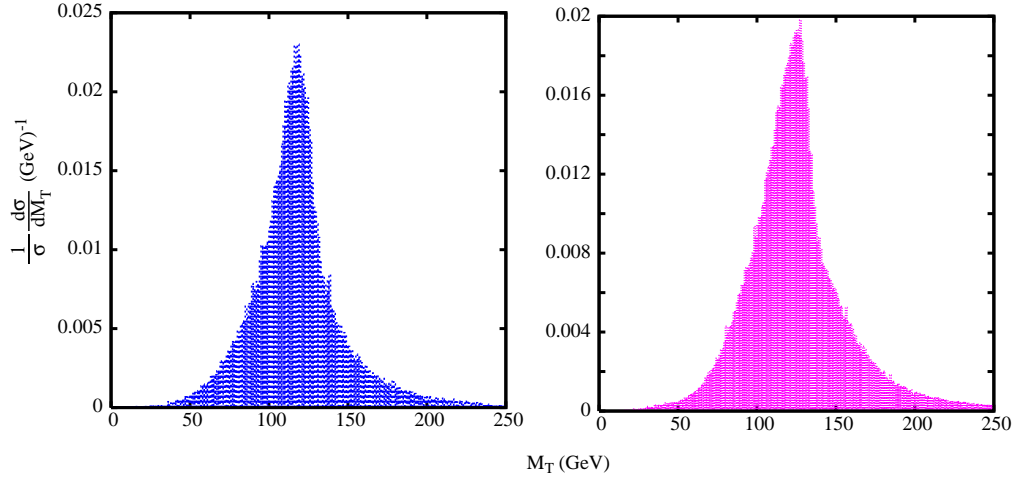


Figure 5: The transverse mass distribution (as defined in the text) for the signal, for $M_{H^\pm} = 129.55$ GeV (left panel) and $M_{H^\pm} = 135$ GeV (right panel), $\tan \beta = 4.5$ and $\Phi_{CP} = 90^\circ$.